LETTER • OPEN ACCESS

# Boundary-induced pattern formation from temporal oscillation: Spatial map analysis

To cite this article: Takahiro Kohsokabe and Kunihiko Kaneko 2016 *EPL* **116** 48005

A Letters Journal Exploring the Frontiers of Physics

November 2016

EPL, **116** (2016) 48005
doi: 10.1209/0295-5075/116/48005

www.epljournal.org

# Boundary-induced pattern formation from temporal oscillation: Spatial map analysis

Takahiro Kohsokabe[1] and Kunihiko Kaneko[2]

[1] *Department of Basic Science, Graduate School of Arts and Sciences, The University of Tokyo 3-8-1 Komaba, Meguro, Tokyo 153-8902, Japan*
[2] *Research Center for Complex Systems Biology, Graduate School of Arts and Sciences, The University of Tokyo 3-8-1 Komaba, Meguro, Tokyo 153-8902, Japan*

received 23 August 2016; accepted in final form 20 December 2016
published online 9 January 2017

PACS 82.40.Ck – Pattern formation in reactions with diffusion, flow and heat transfer
PACS 47.54.-r – Pattern selection; pattern formation
PACS 05.65.+b – Self-organized systems

**Abstract** – Boundary-induced pattern formation is investigated using spatially one-dimensional, two-component reaction-diffusion equations. Temporal oscillation is successively transformed into a spatial pattern, triggered by diffusion from the fixed boundary. We introduced a spatial map, whose temporal sequence, under selection criteria from multiple stationary solutions, can completely reproduce the emergent pattern, by replacing the time with space. The relationship of the pattern wavelength with the period of oscillation is also obtained The pattern wavelength is proportional to the period of the oscillation when the emergent pattern is periodic. The generality of the pattern selection process and algorithm is discussed with possible relevance to biological morphogenesis.



**Introduction.** – Spatial patterns are ubiquitous in non-equilibrium systems, and the process of spontaneous pattern formation has been extensively studied as one of the main issues in non-linear dynamics. Topic areas in pattern formation include fluid, solid-state, optical, geophysical, chemical, and biological systems [1–5].

In particular, the reaction-diffusion system, which was pioneered by Turing [6], has been a focus of non-equilibrium studies. In his celebrated study, Turing showed how a spatial pattern or temporal rhythm is spontaneously formed from a spatially homogeneous and temporally stationary state, which is unstable against perturbations. Turing classified such pattern formation processes into six cases, one of which is known as the *Turing pattern*, a stationary periodic pattern with the finite wavelength given by linear stability analysis. While Turing originally proposed his theory as a model of morphogenesis, it has been applied to general pattern formation dynamics beyond developmental biology [7,8].

Turing also noted that, in a reaction-diffusion system, spontaneous pattern formation from temporally dynamic states is also possible. [6]. Destabilization of a spatially homogeneous and temporally oscillatory state by diffusive interaction often results in spatiotemporal dynamics such as waves, spirals, and turbulence [9]. Spatiotemporal dynamics by combination of Turing instability for pattern formation and Hopf bifurcation for temporal oscillation have been studied as Turing-Hopf bifurcation [10–12].

However, an important factor that has not been fully explored is the influence of boundary conditions on spatial patterns. In particular, pattern formation from temporally dynamic states may be crucially influenced by the introduction of a fixed boundary. The influence may be globally propagated to alter the pattern dynamics. (See also [13,14] for the relevance of boundary conditions in pattern dynamics.)

In the present letter, we are concerned with such boundary-induced pattern formation, namely, how a fixed boundary condition induces pattern formation of spatially non-uniform and temporally fixed pattern, from a temporally periodic and spatially uniform attractor that exists under Neumann or periodic boundary condition.

The question of boundary-induced pattern formation is not only of theoretical interest but also of experimental interest in developmental biology. In the somitogenesis of vertebrate development, temporal oscillation in protein expression is fixed into a spatial pattern [15,16]. In chick development, the gene expression of c-hairy1, which initially oscillates in the presomitic mesoderm, is fixed into a striped pattern along aligned cells. So far, such spatial pattern formation has been studied by introducing external inputs that move in space with time development (*clock and wavefront*) [17]. Diffusive interaction has been introduced by Meinhardt in addition to external input using a spatial gradient [18]. In his theoretical study, the use of an external input is essential to induce formation of spatial inhomogeneous pattern. Some recent experiments, however, suggested that an external input may not be essential, and intrinsic instability due to diffusion might result in somitogenesis [19,20]. If boundary-induced pattern formation is possible without imposing an external input throughout the space, it will provide a plausible mechanism for vertebrate somitogenesis.

Here, we demonstrate that temporal oscillation in a spatially one-dimensional reaction-diffusion system is fixed into a stationary periodic spatial pattern by introducing fixed boundary condition. In this case, in contrast to the celebrated Turing pattern, the wavelength of the generated pattern cannot be obtained using linear stability analysis around the fixed point. Instead, to predict the selected pattern, we introduced a one-dimensional spatial map, whose attractor gives the one-dimensional pattern by replacing time with space. The generality of this oscillation fixation and the pattern selection mechanism will be discussed.

**Results.** – Now, consider a spatially one-dimensional reaction-diffusion system of two components $X$ and $Y$. We assume that the diffusion of $X$ is much faster than that of $Y$, and the diffusion of the latter is neglected for simplicity (the formalism to be discussed is valid even without this approximation). Then, the equation is written as

$$\begin{aligned} \frac{\partial X}{\partial t} &= f(X,Y) + D\frac{\partial^2 X}{\partial x^2}, \\ \frac{\partial Y}{\partial t} &= g(X,Y), \end{aligned} \tag{1}$$

where $f(X,Y)$ and $g(X,Y)$ are the reaction functions for $X$ and $Y$, $D$ is the diffusion constant of $X$, and the attractor of the dynamical system without the diffusion term is a limit cycle[1].

[1]When this limit cycle is generated by a Hopf bifurcation from the fixed point $(X^*, Y^*)$, the eigenvalues of the Jacobi matrix around the fixed point are complex with a positive real part and a non-zero imaginary part, so that $a + d > 0$ and $-2 < \frac{d-a}{\sqrt{-bc}} < 2$ [6], where

$$\begin{pmatrix} a & b \\ c & d \end{pmatrix} = \begin{pmatrix} \frac{\partial f}{\partial X} & \frac{\partial f}{\partial Y} \\ \frac{\partial g}{\partial X} & \frac{\partial g}{\partial Y} \end{pmatrix}_{X=X^*, Y=Y^*}. \tag{2}$$

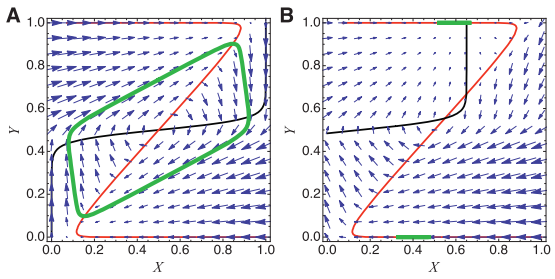


Fig. 1: (Color online) (A) The nullclines $f(X,Y) = 0$ (red) and $g(X,Y) = 0$ (black) as well as the limit cycle orbit (green) are plotted in the state space for the model (2), for the case $D = 0$. Flow in the state space is also illustrated by arrows. (B) State space plot of nullclines of $f(X,Y) + D\frac{\partial^2 X}{\partial x^2}$ (black) and $g(X,Y) = 0$ (red) are plotted at some location $x$. Flow in the state space is also illustrated as arrows. The nullcline of $X$ is shifted horizontally from the $D = 0$ case with the spatial gradient at each location (see also fig. 3). The series of cross-points of the nullclines at $Y \sim 1$ or $Y \sim 0$ at each location give the emergent stationary pattern orbit (green).

We consider the case in which the spatially uniform oscillatory state is stable against perturbations so that under Neumann or periodic boundary conditions, the spatially uniform oscillation is the attractor of the system. On the other hand, under a fixed boundary condition, oscillation in the vicinity of the boundary is strongly suppressed. In the present case, the variable $X$ there reaches a fixed value. This fixation from the uniform oscillatory state propagates downflow (see fig. 2), and a fixed periodic spatial pattern is generated.

As a specific example, consider the following system,

$$\begin{aligned} f(X,Y) &= \frac{1}{1+e^{-\beta(Y-1/2)}} - X, \\ g(X,Y) &= \frac{1}{1+e^{-\beta(Y-X)}} - Y \end{aligned} \tag{3}$$

which describes the protein expression dynamics with two genes, where $X$ inhibits the expression of $Y$ and $Y$ activates the expressions of both $X$ and $Y$ [21,22]. If $\beta > 8$ and $D = 0$, this system has one unstable fixed point $(X^*, Y^*) = (1/2, 1/2)$, and the limit cycle is an attractor (see fig. 1(A)). Indeed, from initial conditions close to a spatially homogenous state, a uniform, limit-cycle state is reached if the boundary condition is of Neumann type or periodic. In contrast, if a fixed boundary condition is adopted for at least one end, *i.e.*, $X(0,t) = X_0$, temporal oscillation is replaced by a fixed pattern[2] (see fig. 2(A) and (B) where $\frac{\partial X}{\partial x}|_{x=L} = 0$ is adopted at the other end). Note that a pattern of the same wavelength is organized independently of $X_0$ as long as $X_0$ is in the range [0, 1] (see fig. 3). Here, initially a uniform oscillatory state exists for $x > 0$. Then, the oscillation ceases in the vicinity of $x = 0$, while the oscillation continues in the free end.

[2]A boundary condition for $Y$ is not required as diffusion in $Y$ is neglected.

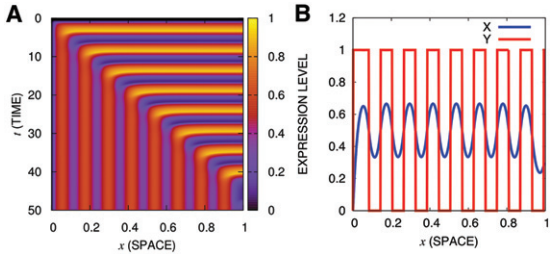


Fig. 2: (Color online) Time development of the model (2) under a fixed boundary condition, $X(0) = 0$. (A) $X(x,t)$ is displayed with a color scale given by the side bar. The abscissa is time $t$, and the ordinate is space $x$. (B) The generated stationary pattern $X(x)$ and $Y(x)$. The abscissa is the concentration of $X(x)$ or $Y(x)$, and the ordinate is space $x$. $\beta = 40$ and $D = 1.6 \times 10^{-3}$.

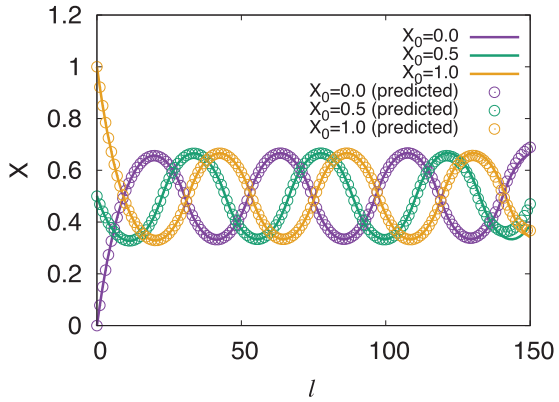


Fig. 3: (Color online) Stationary pattern $(X_{st}(l), Y_{st}(l))$ of the reaction diffusion (3) and the predicted pattern of $(X_l, Y_l)$ obtained from the spatial map (6). The predicted pattern (given by $\circ$) agrees well with the stationary pattern (lines). Three patterns with boundary values of $X_0 = 0.0$ (purple), $X_0 = 0.5$ (green), and $X_0 = 1.0$ (yellow) are considered. $\beta = 40$ and $D = 4.0 \times 10^{-4}$.

The uniform temporal oscillation, per one period, is replaced by a temporally fixed, spatially periodic pattern with one wavelength, which works as a boundary condition for $(X(x), Y(x))$ for larger $x$. Accordingly, the temporal oscillation is successively replaced by a temporally fixed spatially periodic pattern.

Note that this pattern formation dynamics takes place far from the uniform fixed-point solution. Hence, the standard linear stability analysis for the Turing pattern concerning around the uniform fixed-point solution cannot explain the wavelength observed here. (See supplemental fig. 1 in [23].)

Meanwhile, the emergent stationary pattern has to satisfy

$$\begin{aligned} f(X,Y) + D\frac{\partial^2 X}{\partial x^2} &= 0, \\ g(X,Y) &= 0. \end{aligned} \tag{4}$$

Equation (4) describes nullclines of $X$ and $Y$ of the emergent stationary pattern, at each location. Since the

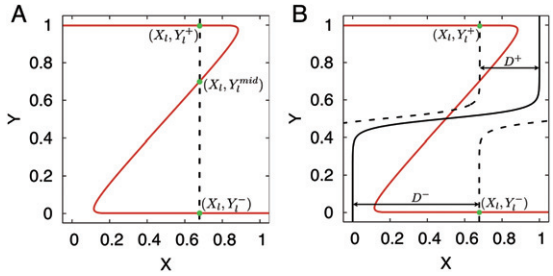


Fig. 4: (Color online) (A) The nullcline of $Y$, given by $g(X,Y) = 0$ (red solid line). Crossing points of $g(X,Y)$ and $X = X_l$ (black dashed line) show candidate solutions of spatial map at $l$ (green circles). (B) State space plot of the nullcline of $Y$ (red solid line) and the nullcline of $X$ when $D = 0$ (black solid line). The two dashed lines are nullclines of $X$ assuming $Y_l = Y_l^+$ (the upper one with the crossing point $(X_l, Y_l^+)$) and that assuming $Y_l = Y_l^-$(the lower one with the crossing point $(X_l, Y_l^-)$). The distance between each dashed lines and the original nullcline $F(X,Y) = 0$ corresponds to the diffusion terms, *i.e.*, $D^+ = D'|X_{l+1}^+ - 2X_l + X_{l-1}|$ or $D^- = D'|X_{l+1}^- - 2X_l + X_{l-1}|$.

nullcline of $X$ is changed by the diffusion term from the original ordinary differential equations, under the diffusion term $D\frac{\partial^2 X}{\partial x^2}$, novel fixed points can appear.

At each location, crossing-points of two nullclines indicate such novel fixed points. The stationary pattern is described as the chain of such novel fixed points along the space. Actually, for the given stationary pattern, we confirmed that the stationary state $(X,Y)$ is the same as a novel stable fixed point given by the calculated diffusion term at each location (see fig. 4(B)). Thus, under the diffusion term at each location, the stationary pattern is computed.

By adopting spatial discretization, this condition is given by

$$\begin{aligned} f(X_l, Y_l) + D'(X_{l+1} - 2X_l + X_{l-1}) &= 0, \\ g(X_l, Y_l) &= 0, \end{aligned} \tag{5}$$

where $l$ is the discretized space index with $a$ as the discretized unit length, *i.e.*, $x = al$ and $X_l = X(x/a)$, $Y_l = Y(x/a)$. Here, $D'$ is the rescaled diffusion constant which satisfies $D' = D/a^2$. From these equations, we can derive the spatial map as follows:

$$\begin{aligned} X_{l+1} &= 2X_l - X_{l-1} - \frac{f(X_l, Y_l)}{D'}, \\ Y_l &= g_{X_l}^{-1}(0), \end{aligned} \tag{6}$$

where $g_{X_l}^{-1}$ is the inverse function of $g(X,Y)$ given that $X$ is fixed to $X_l$, which corresponds to the cross-points of the two nullclines. With these equations, $X_{l+1}$ can be determined from $X_l$, $Y_l$ and $X_{l-1}$, while $Y_l$ is determined as $g_{X_l}^{-1}(0)$ (for the use of a "spatial map" in the analysis of a spatial pattern, see also [24,25]). Hence the spatial pattern is determined as a time-series of the mapping (6), by replacing $l$ into the spatial sequence.

Here, however, multiple branches in the solution can exist for $Y_l = g_{X_l}^{-1}(0)$, as shown in fig. 4(A). All of these give potential, stationary solutions, but not all of the candidate solutions $(X_l, Y_l)$ are stable in terms of dynamical systems (1). In addition to the stability, we need to choose such solution that is attracted from the (vicinity of) spatially homogeneous initial condition. These properties give constraint on the selection of the branch $Y_l = g_{X_l}^{-1}(0)$. (As will be argued in the "Discussion" section, different patterns could be reached starting from the initial condition far from uniformity, which are realized as a different choice of the branches from those below. Note that the attractor reached from the vicinity of the uniform initial condition is unique.)

Consider the case of eq. (3). Figure 4(A) shows the candidate solutions at a given $l$. There are three candidate solutions of $Y_l$, namely $Y_l^+, Y_l^{mid}$ and $Y_l^-$, given by different branches of $g_{X_l}^{-1}(0)$. Here, $(X_l, Y_l^{mid})$, which comes from the original unstable fixed point in eq. (3), is an unstable fixed point, as can be directly seen in the flow in fig. 1(B) (see also the supplementary text in [23]). Thus, there remain two candidates for the emergent stationary pattern, *i.e.*, $(X_l, Y_l^+)$ or $(X_l, Y_l^-)$. Both these candidate solutions are stable fixed points, as seen in fig. 1(B) and analyzed in the supplementary text in [23].

Then, the constraint that the fixed point at $(X_l, Y_l)$ is attracted from a uniform oscillatory state under the boundary condition determines the solution to be selected: Since the pattern emerges from a uniform state and $X$ is under diffusion to homogenize the solution, such solution with a smaller diffusion term $|X_{l+1} - 2X_l + X_{l-1}|$ should be selected. From eq. (5), this diffusion term is given by $|f(X_l, Y_l)|$, which is identical to the distance from the original nullcline of $X$, *i.e.*, $f(X, Y) = 0$. Then, as shown in fig. 4(B), once a given branch (say $Y^+$) is selected, the diffusion term $|X_{l+1}^+ - 2X_l + X_{l-1}|$ is smaller than that of the other branch (*i.e.*, $|X_{l+1}^- - 2X_l + X_{l-1}|$), up to a certain lattice point $l^*$ (to be shown below). Due to the continuity of $\frac{\partial^2 X}{\partial x^2}$, the solution at the same branch (say, $Y_{l+1}^+$) will be selected at the next location (see fig. 4(B)). Now, by taking the same branch (say + in fig. 4(B)), $|f(X_l, Y_l)|$, and accordingly, the distance between $(X_l, Y_l)$ and the original $X$-nullcline increases. Then, at a certain lattice point $l = l^*$, $|f(X_l, Y_l^+)|$ turns to be equal to $|f(X_l, Y_l^-)|$, beyond which the latter is smaller. Hence, beyond $l = l^*$, $|X_{l+1}^+ - 2X_l + X_{l-1}|$ exceeds $|X_{l+1}^- - 2X_l + X_{l-1}|$. Then. $Y_l^+$ is no longer selected but $Y_l^-$ is selected, due to the proximity to uniformity.

Here it should be noted that by the original dynamics given by eq. (3), $(X, Y)$ moves along the limit cycle attractor. Then starting from $(X_l^+, Y_l^+)$, $(X, Y)$ is directed toward $(X_l^-, Y_l^-)$. Hence the − branch of the solution that gives rise to a smaller diffusion term is accessible by the original dynamics, so that the selected branch switches from + to −. Then, the minus branch remains to be selected due to the continuity, until $|X_{l+1}^- - 2X_l + X_{l-1}|$ exceeds $|X_{l+1}^+ - 2X_l + X_{l-1}|$. Repeating the above procedure, the emergent periodic pattern is predicted.

Since the present model has point symmetry with respect to $(X, Y) = (0.5, 0.5)$, the condition for the selection of the solution branch is simply written as

$$Y_l = \begin{cases} Y_l^+ & (|D'(X_{l+1}^+ - 2X_l + X_{l-1}| < 0.5), \\ Y_l^- & (\text{otherwise}). \end{cases} \quad (7)$$

An example of the pattern obtained from the spatial map with the above selection criterion is shown in fig. 3, which completely agrees with the numerically obtained pattern. The above procedure works independently of the parameter values, demonstrating its validity.

Note that the spatial periodic pattern is obtained as an attractor of the spatial map (6). Hence, independently of the initial condition in the map, the same periodic pattern is selected as long as the initial condition in the spatial map belongs to the basin of the above attractor. The initial condition in the spatial map corresponds to the value of the fixed boundary. Hence, a pattern of the same wavelength is reached independently of the boundary value, while the phase of the wave pattern is different, which is consistent with the numerical result (see fig. 3).

This procedure also suggests that there can be a relationship between the period of oscillation $T$ and the wavelength $\lambda$. First, by rescaling the spatial scale, the wavelength $\lambda$ is proportional to $\sqrt{D}$. (The period is scaled by $\tau$ if $f$ and $g$ are similarly scaled by $1/\tau$, but this is already set to unity in (1).) Then, we have found $\lambda/\sqrt{D} \propto T$. In fact, we numerically confirmed that one stripe is generated in correspondence with one period of oscillation from a uniform limit-cycle state in the free end, except for the vicinity of the Hopf bifurcation (see fig. 2(A)).

Now, following the vector field $(f(X, Y), g(X, Y))$ in the state space (see fig. 1(A)), $(X(t), Y(t))$ oscillates with the period $T$. Here, within one period of oscillation, $f(X, Y)$ increases and takes a local maximum, and decreases to change the sign, and then takes a local minimum, and increases to change the sign, as in the state space in fig. 1(B).

On the other hand, when a stripe is formed, the "spatial orbit" $(X(x), Y(x))$ against $x$ is shaped within the state space. Recalling that the switch to the other branch occurs when $|f(X, Y)|$ takes a local maximum, $f(X, Y)$ changes along with the spatial sequence as follows: By starting from the + branch, $f(X, Y) > 0$ decreases to take the local minimum, and then increases to take a local maximum, and then $f(X, Y)$ switches its sign. Entering the − branch, $|f(X, Y)|$ first decreases to a local minimum, and then increases to take the local maximum to switch to the + branch. Hence, although the timing of the sign change is different, $f(X, Y)$ and its derivative experiences one cycle of sign change both through the limit cycle and spatial orbit.

With the parameter change, the magnitude of a vector $(f, g)$ in the state space changes, which alters the angular

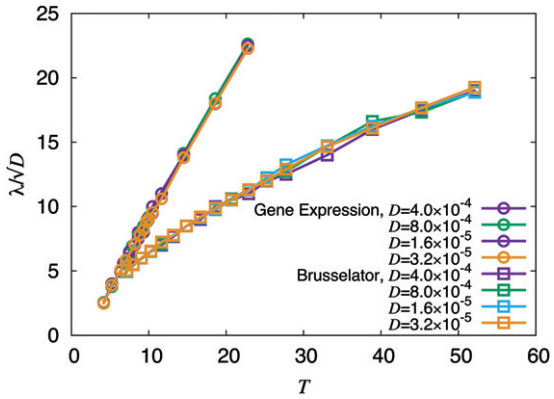


Fig. 5: (Color online) Relationship between the scaled wavelength $\lambda/\sqrt{D}$ of the emergent pattern and the period of the limit cycle orbit $T$ is shown by changing parameter $\beta$. Results from different $D$ values are also plotted with different symbols. The relationship from the Brusselator equation (8) is also plotted from the obtained data by varying $B$. $A$ is fixed to 1.

velocity along the limit cycle as well as that of the "spatial orbit" in the same way. Hence, the period $T$ and wavelength $\lambda$ (or $\lambda/\sqrt{D}$) change in proportion. Of course, this is a rough estimate, but this proportionality approximately holds against changes in the parameter values $\beta$ (and $D$), as shown in fig. 5.

For smaller values of $\beta$, the deviation from the proportionality is discernible, where the spatial pattern exhibits period-doubling (see supplementary fig. 2 in [23]). For a much smaller value of $\beta$, the pattern predicted by the spatial map can be quasiperiodic or chaotic, where, however, such spatial pattern that is fixed in time turns to be unstable in the time evolution of the original reaction-diffusion dynamics. Then, the attractor is no longer a fixed point in time but is replaced by spatiotemporal dynamics.

The fixation of the temporal to the spatially periodic pattern as well as the analysis using the spatial map can be generally applied to a spatially one-dimensional reaction-diffusion equation that has a uniform limit-cycle attractor. As another illustration, we have also examined the so-called Brusselator [1]:

$$\begin{aligned} f(X,Y) &= BY - XY^2, \\ g(X,Y) &= A - (B+1)X + XY^2. \end{aligned} \tag{8}$$

In this case, a uniform periodic oscillation is replaced by a spatial pattern by applying the fixed boundary condition $X(0) = X_0$, for a certain range of parameters. The selection of the branch for $Y_l$ in the spatial map is much easier for this case than eq. (3). One can just choose the same branch as long as the branch exists and it is in the basin of the limit cycle, *i.e.*, the solution satisfies $X_l > 0$ and $Y_l > 0$. In fact, the switch of the branch due to the selection of smaller $|X_{l+1} - 2X_l + X_{l-1}|$ need not be taken into account in this case, since the flow in the state space goes toward the fixed point of the original branch, and the switch cannot occur starting from the limit-cycle attractor (this is because the rotation along the limit cycle of the Brusselator model is counterclockwise).

Again, the pattern predicted through spatial map and the above selection criteria of branches agrees well with the emergent pattern (see supplemental fig. 3 in [23]). The approximate proportionality between the period and wavelength is worse than the model (2) (see fig. 5), possibly because the correspondence between the flows in the spatial map and original limit cycle is not so good in the state space.

**Discussion.** – In the present letter, we have studied the formation of a periodic pattern from a uniform oscillatory state induced by the boundary conditions. The emergent pattern is predicted as an attractor of the spatial map under the selection principle. We have confirmed the generality of this pattern formation in reaction-diffusion systems. The periodic oscillation exists in a two-component reaction system with negative feedback. That is, in a system with an activator and an inhibitor, for a certain range of parameters, there exists an oscillatory attractor. Under a fixed boundary condition, this state is replaced by the spatially periodic, temporally fixed state, if the diffusion of the inhibitor is sufficiently large.

We also note that the pattern formation process as well as the nullcline analysis is still valid even for $D_Y \neq 0$. As long as $D_Y$ is small, the present stripe formation will be preserved under perturbative analysis. The analysis of the spatial map can be applicable generally, although the inverse function that includes both $X$ and $Y$ would make the analysis more difficult.

Pattern formation generally depends on the boundary and initial conditions. In the spatial map, the former is represented by the initial condition in the map, while the latter is considered by the proximity to uniformity, which indicates that the initial condition is not far from the uniform oscillatory state. If the initial condition is far from uniformity, local inhomogeneity can grow. In the state-space representation, whether such growth occurs is determined according to the size of the spatial diffusion term, specifically whether the spatial diffusion term is large enough to go across the nullclines and to induce a switch to the other branch. In other words, the condition close to uniformity represents the absence of such inhomogeneity.

On the other hand, for such initial conditions that allow the local growth in inhomogeneity, the selection criterion of the solution branch is the proximity to a given initial condition, which leads to a requested switch to a different branch of fixed-points. In other words, the choice of the fixed-point solution corresponding to the initial condition can predict the emergent pattern. Conversely, control of an emergent pattern is thus possible by manipulating the initial condition.

Experimental confirmation of the present pattern formation will be possible in reaction-diffusion systems. In particular, relevance of boundary condition to pattern

selection should be of importance because the real experimental system is finite and often under a fixed boundary condition. By carefully examining the boundary effects, we can confirm the present pattern formation mechanism, where the period-wavelength relationship (fig. 5) will be confirmed.

As mentioned in the introduction, spatial pattern formation based on temporal oscillation is often observed in biological morphogenesis [15,16] as well as in the numerical evolution of morphogenesis [26,27], where the relevance of cell-cell interaction has recently been discussed [20,27]. Considering the simplicity in our mechanism, which only requires diffusion of the inhibitor and a fixed boundary, we expect that it could be adopted in biological development, which will be confirmed by examining cell-cell interaction and boundary effects.

* * *

The authors would like to thank Nen Saito for useful discussions. This work was partially supported by the Platform for Dynamic Approaches to Living Systems from AMED, Japan.

REFERENCES

[1] Nicolis G. and Prigogine I., *Self-organization in Nonequilibrium Systems* (John Wiley & Sons, New York) 1977.
[2] Cross M. C. and Hohenberg P. C., *Rev. Mod. Phys.*, **65** (1993) 851.
[3] Walgraef D., *Spatio-temporal Pattern Formation with Examples from Physics, Chemistry and Materials Science* (Springer) 1997.
[4] Winfree A. T., *The Geometry of Biological Time*, Vol. **12** (Springer Science & Business Media) 2001.
[5] Kapral R. and Showalter K., *Chemical Waves and Patterns*, Vol. **10** (Springer Science & Business Media) 2012.
[6] Turing A. M., *Philos. Trans. R. Soc. London, Ser. B: Biol. Sci.*, **237** (1952) 37.
[7] Segel L. A. and Jackson J. L., *J. Theor. Biol.*, **37** (1972) 545.
[8] Lenfyel I. and Epstein I. R., *Science*, **251** (1991) 650.
[9] Kuramoto Y., *Chemical Oscillations, Waves, and Turbulence*, Vol. **19** (Springer Science & Business Media) 2012.
[10] De Wit A., Lima D., Dewel G. and Borckmans P., *Phys. Rev. E*, **54** (1996) 261.
[11] Meixner M., De Wit A., Bose S. and Schöll E., *Phys. Rev. E*, **55** (1997) 6690.
[12] Baurmann M., Gross T. and Feudel U., *J. Theor. Biol.*, **245** (2007) 220.
[13] Pomeau Y. and Zaleski S., *J. Phys.*, **42** (1981) 515.
[14] Fujimoto K. and Kaneko K., *Phys. Rev. E*, **63** (2001) 036218.
[15] Palmeirim I., Dubrulle J., Henrique D., Ish-Horowicz D. and Pourquié O., *Dev. Genet.*, **23** (1998) 77.
[16] Pourquie O., *J. Anatomy*, **199** (2001) 169.
[17] Cooke J. and Zeeman E. C., *J. Theor. Biol.*, **58** (1976) 455.
[18] Meinhardt H., *Models of Biological Pattern Formation*, Vol. **6** (Academic Press, London) 1982.
[19] Dias A. S., de Almeida I., Belmonte J. M., Glazier J. A. and Stern C. D., *Science*, **343** (2014) 791.
[20] Cotterell J., Robert-Moreno A. and Sharpe J., *Cell Syst.*, **1** (2015) 257.
[21] Mjolsness E., Sharp D. H. and Reinitz J., *J. Theor. Biol.*, **152** (1991) 429.
[22] Goto Y. and Kaneko K., *Phys. Rev. E*, **88** (2013) 032718.
[23] Supplementary Material: `https://drive.google.com/file/d/0BxIj8cjinuS0SWZUbjhqSi1hS1U/view`.
[24] Aubry S., *The New Concept of Transitions by Breaking of Analyticity in a Crystallographic Model*, in *Solitons and Condensed Matter Physics* (Springer) 1978, pp. 264–277.
[25] Willeboordse F. H. and Kaneko K., *Physica D: Nonlinear Phenom.*, **86** (1995) 428.
[26] Fujimoto K., Ishihara S. and Kaneko K., *PLoS ONE*, **3** (2008) e2772.
[27] Kohsokabe T. and Kaneko K., *J. Exp. Zool. Part B: Mol. Dev. Evol.*, **326** (2016) 61.